

Convective Boiling of R-134a on an Enhanced Tube Bundles

Evraam Gorgy,^{1,*} Steven Eckels,²

¹ Wolverine Tube Inc., Decatur, AL, USA

² Mechanical and Nuclear Engineering, Kansas State University, Manhattan, KS, USA

* Corresponding author. E-mail:Evraam.Gorgy@wlv.com

The current paper presents the experimental investigation of the heat transfer performance and effect of tube pitch on highly enhanced surfaced tube bundles. The fluid-tube combination used was R-134a and enhanced tube TBIIHP. Three pitch-to-diameter ratios were studied 1.167, 1.33, and 1.5; all with a staggered triangle arrangement. Twenty enhanced tubes were used in each bundle; the tube outer diameter and length are 19.05 mm (3/4 inch) and 1 m (39.36 inch), respectively. Three input variables were studied: heat flux (5-60 kW/m²), mass flux (15-55 kg/m².s), and quality (10-70%). The test saturation temperature was 4.44 °C. A local method employing the EBHT technique was implemented in data reduction. All tube bundles showed strong dependency on heat flux. The smallest P/D bundle showed a considerably lower performance than the other two. When compared to the pool boiling performance, the smallest P/D bundle was lower while the other two showed a closer performance. The P/D 1.33 bundle outperforms P/D 1.167 bundle and provide quite similar performance to the P/D 1.5. When considering the refrigerant charge the P/D 1.5 uses compared to the P/D 1.33 bundle, the latter proves to be the optimum.

Introduction

The current paper presents a study of the heat transfer performance of enhanced tube bundles. This research project was funded by ASHRAE (RP-1316). The type of analysis used in this research is based on local measurements. Specifically, four instrumented tubes included in the bundle are used to determine local heat transfer coefficients. Three tube pitches with staggered triangular arrangement of 20 tubes each were studied those are P/D 1.167, P/D 1.33, and P/D 1.5. The application of this research is in design of flooded refrigerant evaporators, which have wide impact in the HVAC&R industry. A typical application for the flooded evaporators is high capacity centrifugal chillers.

A flooded evaporator is a shell and tube heat exchanger in which a fluid circulates inside the tube bundle and is cooled by a refrigerant circulating in the shell and over the tube bundle. Cooling takes place through boiling (phase change) of the refrigerant. In flooded evaporators, the refrigerant flows over the tube bundle from the bottom up; it enters the shell at a thermodynamic quality near 10%, due to the expansion device, and leaves at 100% quality

(saturated vapor). This application is usually called “shell boiling.” The tubes used in these bundles can be smooth or enhanced.

The goal of the current study is to investigate the effect of heat flux, mass flux and quality on the heat transfer performance of flooded refrigerant evaporators utilizing highly enhanced tubes in the three staggered-configuration tube pitches. The primary outcome is the local heat transfer coefficient in the bundle. The leading global variables for designing flooded refrigerant evaporators are heat duty, mass flux, tube arrangement, and tube pitch. Within the tube bundle, variables like heat flux and quality vary considerably. The test matrix was set up as a three dimensional matrix (5×6×4), where the number of points corresponds to the input variables as shown in Table 1.

Table 1 Test matrix inputs

<i>Mass flux (kg/s.m²)</i>	15	20	25	35	45	55
<i>Heat flux (kW/m²)</i>	5	15	30	45	60	
<i>Inlet Quality</i>	0.10	0.35	0.55	0.70		

Background

Boiling on a tube bundle has been in use for decades and has many applications: fire tube steam boilers, kettle re-boilers, waste heat boilers, and flooded refrigerant evaporators. The possible heat transfer regimes of the flooded evaporator from bottom to top are as follows: convective heat transfer, sub-cooled boiling, nucleate boiling, sliding bubbles evaporation, and film boiling. In some cases, the top tubes may experience dry-out. The types of tubes used in flooded refrigerant evaporators are smooth, integral fin, and enhanced. Recently, enhanced tubes have been the focus of many research projects because of their high efficiency. Furthermore, enhanced tube technology has been on the rise as machining techniques continue to advance, previously an obstacle to developing these tubes.

Among those who provided tube bundle reviews are Ribatski and Thome (2007), Webb (2005), Casciaro and Thome (2001) Part 1, Browne and Bansal (1999), Thome (1998), Thome (1996), Collier and Thome (1996), Thome (1990), Jensen and Hsu (1988). Three variables have the most significant effect on the heat transfer coefficient (often referred to as “bundle performance”): heat flux, quality, and mass flux. Those variables are also the center of the analysis of the current study. Notably, Fujita et al. (1986), Memory et al. (1992), and Memory et al. (1994) studied boiling over smooth and enhanced tube bundles in a pool of liquid. However, this is considered a different application than that in the current study, since it does not present the effect of mass velocity on convective boiling; in some cases, the calculation of quality is not possible. Therefore, the effect of quality cannot be assessed.

The following studies point out the effect of tube pitch, or tube spacing, on boiling performance over a tube bundle, which is the focus of the current study. This section is divided into two: studies about the effect of tube spacing in a bundle submerged in a pool of liquid at all times and the studies about the effect of tube pitch for tube bundles under forced convection.

Effect of tube pitch for submerged tube bundles

Liao and Liu (2007) studied boiling of water over a smooth tube bundle at atmospheric and sub-atmospheric pressures focusing on the effect of tube spacing and tube positioning on bundle performance. For sub-atmospheric pressure, the optimum tube spacing is between P/D 1.0556 and 1.0277, and when P/D reaches 1.1112, the effect of tube position becomes apparent. When P/D is less than 1.0556, tube position becomes insignificant. Also, bundle pressure has an effect on the optimum spacing.

Liu and Liao (2006) used the same test facility and test conditions as their previously mentioned study. In this study, and in the one above, they tested in-line vs. staggered tube bundle configuration. At atmospheric pressure, the in-line tube bundle had better performance than the staggered tube bundle.

Qiu and Liu (2004) studied the effect of tube spacing, tube positioning, and bundle pressure on boiling of water over a smooth tube bundle and reported that P/D 1.0166 had the best heat transfer performance at low and moderate heat fluxes. For higher tube spacing, the tube position had a significant effect on heat transfer. For the tightest tube pitch, the heat transfer performance increased with the increase of pressure. Also, Liu and Chen (2001) presented a study similar to the previously mentioned study (Qiu and Liu (2004)). In addition, they investigated the differences between falling film and flooded type evaporators, discovering that flooded evaporators show better heat transfer performance.

Liu and Qiu (2004a) and Liu and Qiu (2002) presented experimental results for boiling of water/salt mixture on smooth tube and roll-worked enhanced tube bundles (the latter is similar to the Wolverine Turbo B). The goals of this study, however, included the effect of tube spacing and tube position within the bundle. The smooth tube results were the same as in their study above, while for the enhanced tube bundle, tube position did not show any difference from the heat transfer perspective. Also, the tight spacing provided heat transfer enhancement for the enhanced tube bundle.

In another study by Liu and Qiu (2004b) using the same test facility and methods but with R-11 as the working fluid, they reported that the P/D has an optimum value of 1.0277 (not the tightest pitch) for best performance

enhancement. Liu and Tong (2002) presented similar work to Liu and Qiu (2004) in addition to producing a model for predicting the CHF, which agreed well with the experimental results.

Effect of tube pitch for tube bundles under forced convection

Gupta (2005) studied the effect of tube position for saturated water boiling over a 5×3 (P/D 1.5) in-line tube bundle and other tube arrangements (P/D 3.0, 4.5, and 6.0) and reported that at low heat flux, the mass flux was significant and diminished as the heat flux increased. Concerning the effect of P/D, Gupta found that the bundle heat transfer coefficient increased as the tube spacing decreased.

Fujita and Hidaka (1998) studied boiling of R-113 over in-line and staggered smooth tube bundles based on two tube pitches for each bundle configuration, P/D 1.3 and 1.5. They reported no significant effect on the heat transfer coefficient due to changing the tube pitch.

Jensen et al. (1992) conducted an experimental investigation of smooth and enhanced tube bundles. The enhanced tubes used in the analysis were smooth, Turbo B, and HIGHFLUX tubes with R-113 as the working fluid, and the two P/Ds used were 1.17 and 1.5. The effect of tube pitch on the smooth tube bundle was significant at low heat flux and high mass flux. Also, the effect of the change of mass flux and quality was negligible for the enhanced tube bundles.

Dowlati et al. (1990) studied void fraction and friction pressure drop of two phase flow of air-water across in-line tube bundles for P/D 1.3 and 1.75. This type of research is known as “adiabatic two-phase flow”. Dowlati et al. reported that void fraction does not show strong dependency on tube pitch; increasing the pitch increases two phase pressure drop. Ultimately, the presented void fraction and two-phase friction multiplier predicted the bundle pressure drop for R-113.

Jensen et al. (1989) studied the effect of tube geometry on a smooth tube bundle testing in-line and staggered tube bundles with P/D 1.3 and 1.7 for each tube bundle. They reported that at low heat flux, the higher tube pitch showed a higher heat transfer coefficient, while at medium heat flux, the heat transfer coefficient showed insignificant dependency on tube pitch.

Hsu and Jensen (1988) studied boiling of R-113 on a stainless steel smooth tube bundle testing different tube pitches to document the effect on heat transfer performance. The tube arrangement was an in-line tube bundle, with two P/Ds, 1.3 and 1.7. They reported that at high heat flux range, the high pitch bundle had the highest heat transfer coefficient while at medium heat flux range, the effect of tube pitch did not appear to be significant. Finally, the

change of mass flux and saturation pressure had a negligible effect on the heat transfer coefficient for the different tube pitches.

Mueller (1986) studied boiling of R-11 over a finned tube bundle with different tube spacing and reported that tube spacing had little effect on heat transfer for the fully developed boiling regime, while tube pitch had considerable effect at the nexus between natural convection and nucleate boiling.

The above mentioned studies show that the effect of tube pitch on enhanced tubes under convective boiling has not yet been addressed. Also, for the studies focused on effect of tube pitch on submerged tube bundles, small tube spacing provided better heat transfer enhancement. Finally, for the studies of smooth tube bundles under convective boiling, results fluctuated between enhancing performance and having an insignificant effect.

Experimental apparatus

The refrigerant is driven by a positive displacement pump in the test facility. The tube bundle was set up in the test section, the main component of the test facility, which is located at the highest point of the test facility. The test facility was also designed to test low pressure refrigerants (R-123); therefore, the height of the test section was set to provide the required net positive suction head (NPSH) for the refrigerant pump, which was proven to be a design constraint for R-123. The R-123 testing and results will be presented in a future publication. The refrigerant leaving the test section flows to the condenser, the refrigerant pump, and completes the circuit with the pre-boiler as shown in Figure 1. The test section is water heated; in which, water circulates throughout the test section and a secondary heat exchanger (the heat source to the test section).

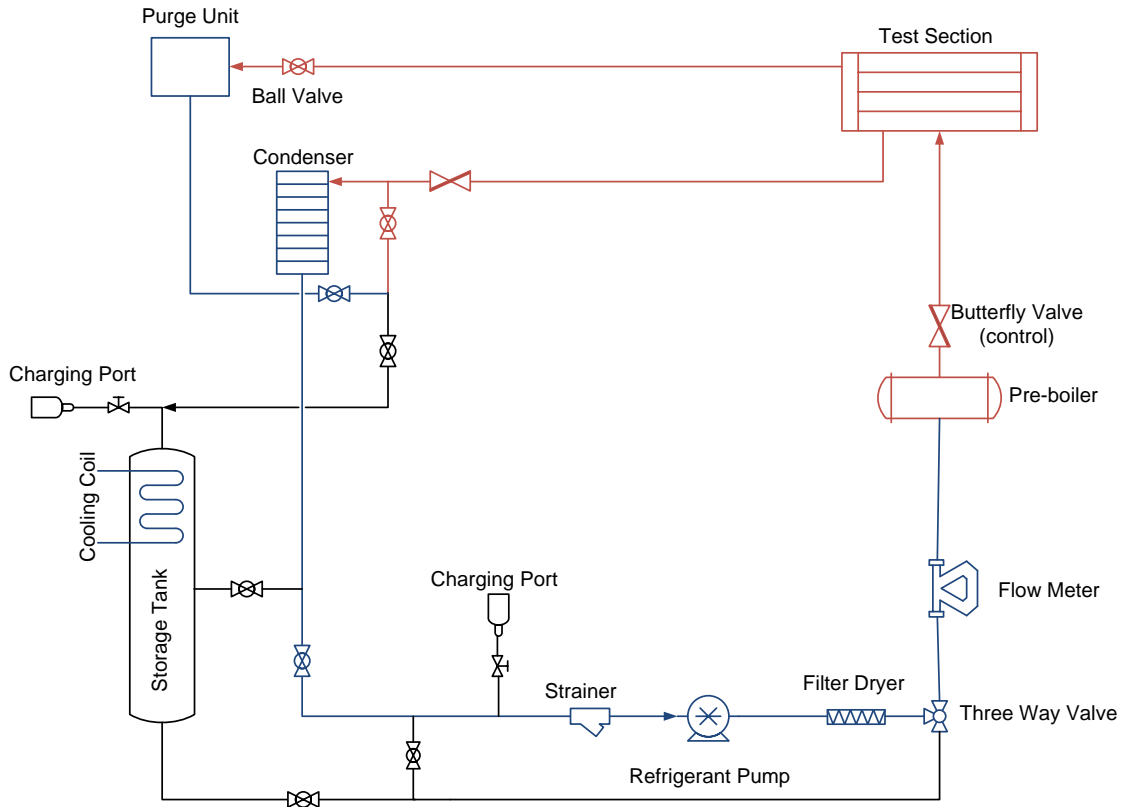


Figure 1 Schematic diagram of refrigerant circuit

Test section

The test section is a rectangular pressure vessel, that is essentially a rectangular-shape shell and tube heat exchanger; the refrigerant flows up through the tube bundle while water circulates in the tubes (see Figure 2). The test section vessel was designed to accommodate more than one tube pitch (see Figure 3). Variable thickness sides (plates) are installed to provide the necessary dimension adjustment for each tube pitch. Additionally, the inside plates are used for mounting half dummy tubes. The half dummy tubes create symmetry for the refrigerant flow around the tubes and simulate an actual evaporator, i.e. making one side a mirror image of the other. The test section has four sight glasses, two on each side which provided a full view of the tube bundle covering the refrigerant inlet up to the top of the tube bundle. The tubes and steel endplates are sealed together by expanding the copper tubes, which is known as tube rolling.

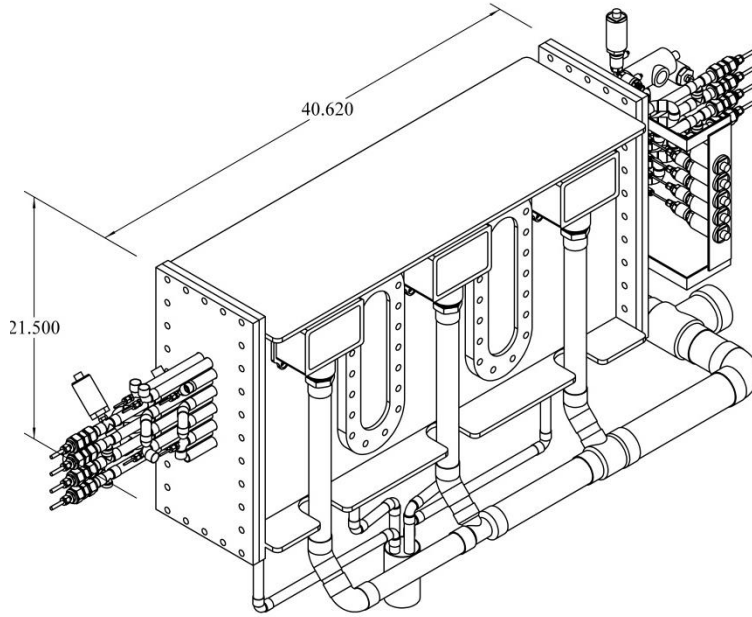


Figure 2 Test section overall dimensions

Refrigerant enters the tube bundle via 8 inlet ports, equally spaced along the length of the test section. The ports are aimed downward, opposite to the flow direction, to reduce the flow kinetic, thus making the vapor equally distributed. In addition, four dummy tubes having the same diameter and tube pitch as the active tubes are swaged in the endplates. Meanwhile, refrigerant exits the tube bundle through rollover rectangular openings on the sides of the test section. The total number of openings is six, three on each side.

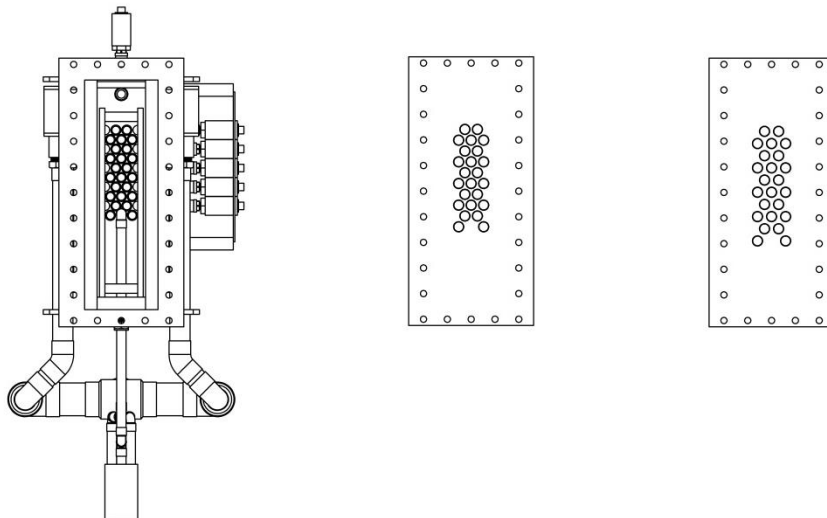


Figure 3 Configuration of the three tube pitches P/D 1.167, 1.33, and 1.5 (left to right)

The water enters the test section at the top of the bundle and is divided into five channels (paths) parallel to each other, it is then sufficient to have the water measurements only on one of the five paths. This instrumented path was

chosen to be the middle tube of the three-tube-set at each row, and was given the name “A.” The water measurements include temperature and pressure measurements. Temperature drop is measured for each of the four tubes of path “A,” while pressure drop is measured across the first and last tubes; that can also be used for determining the total pressure drop across the four tubes. Heat flux was adjusted in the other four paths to match that of “A.”

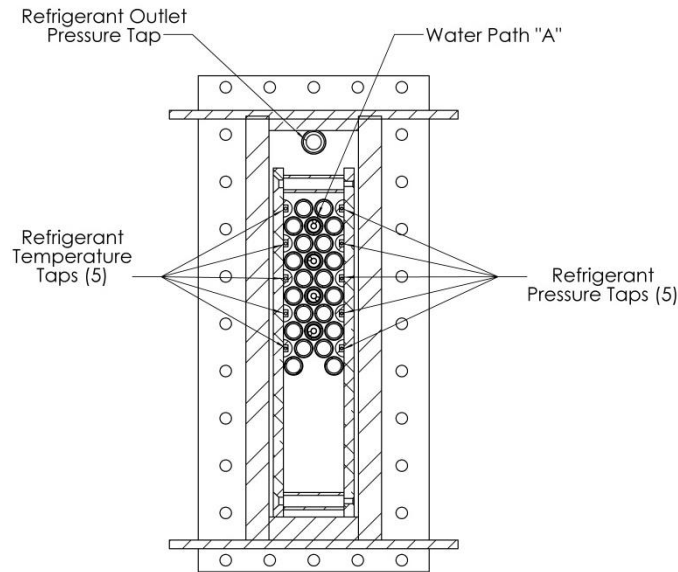


Figure 4 Test section cross sectional view

Instrumented tubes

Total temperature drop in path “A” is determined by measuring the temperature drop in each of the four tubes. An insert tube made of stainless steel wrapped with thick helical cable is placed in the center of each enhanced tube. The insert tube carries seven thermistors, two for measuring the inlet and outlet water temperatures and five internal thermistors for determining the local parameters. Details about the insert tube are mentioned in the next subsection. The thermistors were manufactured in the lab by encapsulating each thermistor in a set screw as shown in Figure 5. The set screw was drilled so that the temperature element is near the tip of the device. Once manufactured, the thermistor probes were calibrated and checked before being affixed to the insert tube. All temperature instruments were calibrated using a constant temperature bath (made by Fluke model 7321) with an uncertainty of ± 0.01 °C and uniformity of ± 0.005 °C. the temperature bath was calibrated using NIST traceable thermometers with a resolution of 0.01 °C. The flow meters used were Coriolis type, which is known for its high accuracy.

Insert tube

The water entering the test section flows within the test tube and over the insert tube (or in between the test tube and insert tube) as illustrated in Figure 5. The insert tube has two purposes: to increase the water velocity and thus the water heat transfer coefficient, and to support the seven thermistors. The higher the water heat transfer coefficient, the more accurate the measured heat transfer coefficient will be because of the better thermal resistance balance. This is tempered by the fact that Wilson Plot can be more difficult. Two of the seven thermistors, the outermost ones, are located outside the heated section and measure the inlet and outlet temperatures of the water. These two probes are axially located in the end-plates of the test section. The advantage of this location is to decrease any inaccuracy of the temperature measurement due to ambient loss. The other five thermistors are evenly distributed along the insert tube. The probe tip was located at the center of the space between the test tube and the insert tube and secured in position by tapping a hole in the insert tube wall and threading the probe to the require depth. The insert tube is centered inside the 1.3 m (51.5 inch) long and 0.01905 m (0.75 inch) nominally wide test tube. Dimensions of the test tubes are provided in Table 2. The tubes are externally and internally enhanced for refrigerant and water, respectively.

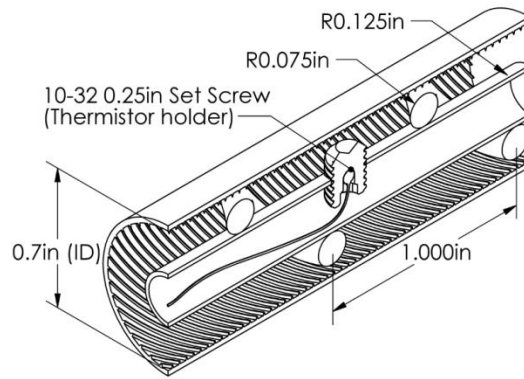


Figure 5 Cross sectional view of test tube and insert tube

Table 2 Enhanced tubes dimensions

	<i>Outside Dia.</i> <i>mm (inch)</i>	<i>Nominal Wall</i> <i>mm (inch)</i>	<i>Fin/inch</i>	<i>Finished fin OD</i> <i>mm (inch)</i>	<i>Inside Root Dia.</i> <i>mm (inch)</i>	<i>Outside Root Dia.</i> <i>mm (inch)</i>
TBIIIHP	19.05 (0.75)	0.635 (0.025)	48	18.69 (0.736)	0.559 (0.022)	17.32 (0.682)

Refrigerant instruments

Temperature and pressure are measured at five levels (heights) in the shell: one at the bundle inlet and four located above the plane of the four instrumented tubes of path “A” as illustrated in Figure 4. Only pressure measurements were used in the analysis; temperature measurements were used only to check the agreement between the temperature and the corresponding saturation temperature determined from the pressure transducers’ measurement (± 0.2 °C was considered acceptable). Temperature probes and pressure transducers are connected to the half dummy tubes installed on the test section’s inside plates.

Data reduction

Tube bundle heat transfer performance is evaluated over a range of heat fluxes, mass fluxes, and other qualities. Particularly, the heat transfer coefficients reported in this study are local to one location in the bundle. The water temperature is measured at five locations in each of the four tubes of the instrumented water path. This data is fit with a second degree polynomial as $T = f(z)$. A finite heat transfer analysis determines the local heat transfer coefficient. Heat is transferred from the water to the cylinder’s inner wall by convection, from the inner wall to its outer wall by conduction, and from the outer wall to the refrigerant by convection (more details in Gorgy and Eckels (2010)).

Consequently, applying conservation of energy and the 1-D heat transfer equations on the finite control volume, assuming no fouling resistance, yields

$$h_w dA_i (T_{hot} - T_{wall,in}) = \frac{2\pi k_c dz}{\ln\left(\frac{D_o}{D_i}\right)} (T_{wall,in} - T_{wall,out}) \equiv dQ \quad (1)$$

and

$$h_r dA_o (T_{wall,out} - T_{cold}) = \frac{2\pi k_c dz}{\ln\left(\frac{D_o}{D_i}\right)} (T_{wall,in} - T_{wall,out}) \equiv dQ \quad (2)$$

where

$$dA_i = \pi D_i dz, \quad (3)$$

and

$$dA_o = \pi D_o dz. \quad (4)$$

Applying Newton’s law of cooling yields

$$dQ = U \cdot dA_o (T_{hot} - T_{cold}). \quad (5)$$

Defining the thermal resistance of the tube wall as

$$R_{wall} = \frac{1}{2\pi dz k_c} \ln\left(\frac{D_o}{D_i}\right). \quad (6)$$

Using Equations (1), (2), (5), and (6), yields the following thermal resistances model

$$\frac{1}{U dA_o} = \frac{1}{h_w dA_i} + \frac{1}{2\pi dz k_c} \ln\left(\frac{D_o}{D_i}\right) + \frac{1}{h_r dA_o}. \quad (7)$$

Substituting Equations (3) and (4) yields

$$\frac{1}{U} = \frac{1}{h_w} \frac{D_o}{D_i} + R'_{wall} + \frac{1}{h_r}. \quad (8)$$

Solving for the heat transfer coefficient h_r , yields

$$h_r = \left(\frac{1}{U} - R'_{wall} - \frac{1}{h_w} \frac{D_o}{D_i} \right)^{-1}. \quad (9)$$

Local heat transfer coefficient

Notably, Equation (9) is length independent. Therefore, all the variables of Equation (9) can be used in the local or average analysis (for example, U_{local} or U_o). To determine the local heat transfer coefficient, Equation (9) is modified to

$$h_{local} = \left(\frac{1}{U_{local}} - R'_{wall} - \frac{1}{h_w} \frac{D_o}{D_i} \right)^{-1}, \quad (10)$$

where U_{local} is the local overall heat transfer coefficient. Following the definition of Newton's law of cooling yields

$$U_{local} = \frac{q''_{local}}{T_{local} - T_{\infty}}. \quad (11)$$

Substituting in Equation (10) yields

$$h_{local} = \left(\frac{T_{local} - T_{\infty}}{q''_{local}} - R'_{wall} - \frac{1}{h_w} \frac{D_o}{D_i} \right)^{-1}. \quad (12)$$

As stated in Equation(12), the local heat transfer coefficient is determined at each local temperature measurement.

Local heat flux

The total heat transfer is determined according to the Enthalpy Based Heat Transfer Analysis (EBHT) introduced in Gorgy and Eckels (2010), which accounts for the effect of pressure change. For the current configuration, the water flow inside the tube experiences large pressure drop. In Equation (12), the local temperature T_{local} and refrigerant temperature T_{∞} are obtained by direct measurements while the local heat flux q''_{local} is determined by the enthalpy change on the differential element as

$$dQ = \dot{m} \cdot di. \quad (13)$$

Assuming incompressible fluid (valid for the current water operating conditions), the finite enthalpy di can be expressed as

$$di = C_p \cdot dT + v \cdot dP. \quad (14)$$

Substituting in Equation (13) and dividing by $\pi \cdot D_o \cdot dz$ yields

$$\underbrace{\frac{dQ}{\pi dz D_o}}_{q''_{local}} = \frac{\dot{m}}{\pi D_o} \left(C_p \frac{dT}{dz} + v \frac{dP}{dz} \right). \quad (15)$$

where dT/dz is determined from

$$T = C_1 z^2 + C_2 z + C_3. \quad (16)$$

The pressure drop term of Equation (15) can be determined by assuming a linear water pressure drop across the tube since the pressure can be determined at the inlet and outlet of each tube. Therefore, dP/dz is reduced to $\Delta P/L$. Pressure drop and temperature slope are determined according to the tube length (1 m). The last necessary component in Equation (12) is the water heat transfer coefficient.

Water heat transfer coefficient

The water flows between the enhanced tube and the insert tube following the swirl shape of the insert tube as illustrated in Figure 5. For flow inside a tube, the heat transfer coefficient for no phase change can be determined using

$$h_i = \frac{Nu_D \cdot k_w}{D_h}, \quad (17)$$

where all the water properties are evaluated at the average inlet and outlet temperatures. For this study the water side Reynolds number varied from 10,000 to 35,000. Since the flow is exclusively turbulent, the Nusselt number can be determined using Gnielinski's correlation (1976) presented as

$$Nu_D = \frac{(f/8)(Re_D - 1000)Pr}{1 + 12.7(f/8)^{1/2}(Pr^{2/3} - 1)}. \quad (18)$$

The entrance region can be ignored because of the presence of the swirls and the turbulent flow. The above correlation, also called the modified Petukhov's correlation (1970), is widely applied in flow inside tubes; Gnielinski's correlation works over a wide range of Reynolds numbers (3000 to 5×10^6) and Prandtl numbers (0.5 to 2000) with accurate results, the friction factor is defined as

$$f = (0.79 \ln(Re_D) - 1.64)^{-2}. \quad (19)$$

The friction factor proposed by Gnielinski in Equation (19) is that of a smooth tube. Since the tubes used are internally enhanced and the pressure drop is measured over each tube, the friction factor can be calculated directly rather than depending on a model

$$f = \frac{\Delta P}{\rho} \cdot \frac{D_h}{L_c} \cdot \frac{2}{V^2}. \quad (20)$$

The internal enhancement of the tubes (micro-fins) and the insert tube's swirls affect accuracy in measuring both the characteristic length and the hydraulic diameter of the above equation. Therefore, the Gnielinski correlation needs a correction factor multiplier, which is determined using the modified Wilson plot technique (Briggs and Young (1969)). Accordingly, the correction factor becomes the leading coefficient of the water heat transfer coefficient as

$$h_w = C_i \cdot h_t. \quad (21)$$

The modified Wilson plot technique was done in a single tube test section as a part of the pool boiling study of this project. Details were published earlier in Gorgy and Eckels (2010) and Gorgy and Eckels (2012). The uncertainty in the water side heat transfer coefficient was dominated by the uncertainty in C_i which was found from the 95% confidence interval of the linear regression.

Local quality

Similar to the local heat transfer coefficient, the local quality is determined at each temperature measurement location (thermistor) and at the minimum flow area between the tubes. The thermodynamic quality is determined by performing an energy balance between the refrigerant side and the water side as

$$\dot{m}_{ref} \cdot \Delta x \cdot h_{fg} = q''_{local} \cdot \pi DL. \quad (22)$$

The test section's 1 m side is theoretically divided into four horizontal planes and five vertical sections, producing 20 control volumes. The test section then becomes a (4×5) matrix. Above each plane (row) lies a group of five tubes; the vertical sections (columns) divide the test section so that the thermistors are centered in each vertical section. Therefore, applying the energy balance on each control volume yields

$$\frac{\dot{m}_{ref}}{5} \cdot \Delta x \cdot h_{fg} = 5 \cdot q''_{local,i,j} \cdot \pi D \frac{L}{5}, \quad (23)$$

or

$$x_{i+1,j} = \frac{5q''_{local,i,j} \cdot \pi DL}{\dot{m}_{ref} \cdot h_{fg}} + x_{i,j}. \quad (24)$$

Since the quality at the bundle bottom is constant at all five locations and equals the test section inlet quality, the quality at each row is determined from the bottom up. The subscript i, j corresponds to (row,column); with the quality at row i and the local heat flux $q''_{local,i,j}$, the quality at the next row $i + 1$ is determined. The local quality (the quality at the minimum cross-sectional area) is calculated by adding the quality entering the instrumented tube to the quality rise due to the local heat flux at the tube centerline. The latter quality is determined by performing an energy balance around the instrumented tube which is in the center of three tubes (i.e. within each of the 20 control volumes). Thus, the energy balance can be expressed as

$$\frac{\dot{m}_{ref}/5}{3} \cdot \Delta x \cdot h_{fg} = \frac{q''_{local}}{2} \cdot \pi D \frac{L}{5}, \quad (25)$$

or

$$x_{local,i,j} = \frac{q''_{local}/2 \cdot \pi DL}{\dot{m}_{ref}/3 \cdot h_{fg}} + x_{i,j}. \quad (26)$$

Mass flux

The mass flux (also called mass velocity) is calculated based on the minimum area between tubes as

$$G = \dot{m}/A_{\min} , \quad (27)$$

where

$$A_{\min,P/D} = ((P/D) \times D - D)(L_T) \text{ m}^2 . \quad (28)$$

Uncertainty analysis

The uncertainty analysis is performed using the Kline-McClintock (1953) second order law. To determine the final uncertainty in the heat transfer coefficient first required defining the input variables uncertainty. The input variables can be the measured variables (temperature, pressure, and flow rate) or the calculated variables such as saturation temperatures, water heat transfer coefficient, and so forth. Table 3 presents the input uncertainties. The water properties were called in Excel from RefProp 8.0 without using curve fit equations. Therefore, the water properties uncertainty is considered negligible.

Table 3 Input uncertainty

$u_T(^{\circ}C/^{\circ}F)$	$\pm 0.015/0.027$	u_m	$\pm 0.1\% \times \text{Reading}$	$u_{wp,low-range}$	$\pm 0.51571 \text{ kPa}/0.075 \text{ PSI}$
$u_{Tsat, R134a}(^{\circ}C/^{\circ}F)$	$\pm 0.022/0.0369$	$u_{wp,high-range}$	$\pm 1.0342 \text{ kPa}/0.15 \text{ PSI}$	u_{hw}	$0.04 \cdot h_w$
$u_{Tsat, R123}(^{\circ}C/^{\circ}F)$	$\pm 0.03/0.054$				

The local heat transfer coefficient uncertainty is determined by applying propagation of error on Equation (29). The uncertainty in all the variables in this equation is given in Table 3, except the local temperature T_{local} and the temperature slope dT/dz . The temperature slope uncertainty was determined using a Monte Carlo simulation which is explained at length in Gorgy and Eckels (2012). The uncertainty of the local temperature is the same as the temperature uncertainty. The analysis showed that the dominant source of uncertainty is the temperature uncertainty; therefore, data at low heat flux presents higher uncertainty than high heat flux data because of the low temperature difference.

$$h_{local} = \left(\frac{T_{local} - T_{sat}}{\dot{m} / \pi D_o \left(C_p \left| \frac{dT}{dz} \right| + v \Delta P / L \right)} - R'_{wall} - \frac{1}{h_w} \frac{D_o}{D_i} \right)^{-1} . \quad (29)$$

Results

Testing was performed at a saturation temperature of 4.44 °C (40 °F) using an enhanced TBIIHP tube. The results are presented as plots of the effect of the variables heat flux, mass flux, and quality on the refrigerant side heat transfer coefficient for the three tube pitches. Those three variables are interrelated, which makes it difficult to determine the change in the heat transfer coefficient with respect to one variable independent of the other two (i.e. the other two held constant). Rather, the range of the other two variables is kept as narrow as possible. Ultimately, the heat flux proves to be the most influential variable for enhanced tubes over the mass flux or quality. That is not an unexpected conclusion since it has also been reported in open literature for enhanced tubes.

The heat transfer coefficient change with respect to heat flux at all tested mass flux and inlet quality ranges for the three P/D ratios was studied. The single-tube pool boiling trend (see Gorgy and Eckels (2010) and (2012) for details) was also included. Figure 6 below illustrates the three bundles comparison. The P/D 1.167 tube bundle has the lowest performance of the three tube pitches; its performance is significantly lower than that of the other two tube pitches and pool boiling. In fact, the heat transfer coefficient of some points is 1.5 times lower than that of the other two tube pitches. P/D 1.33 and P/D 1.5 tube bundles show similar performance; nevertheless, the performance of P/D 1.5 is slightly higher than that of P/D 1.33 since it approaches pool boiling at medium and high heat fluxes. Notably, the number of data points decrease for higher P/D ratios due to capacity limitation of the test facility. Beyond the heat flux mark of 40 kW/m² (12680 BTU/hr.ft²), the trends clearly show that the higher the tube pitch, the closer to the pool boiling performance the bundle behaves. All three bundles show rapid increase of heat transfer coefficient over pool boiling at low heat flux, possibly due to the effect of early pores activation flow boiling exerts. Accordingly, tube pitch effect on bundle performance is conducted by comparing the heat transfer coefficient vs. heat flux plots of each bundle.

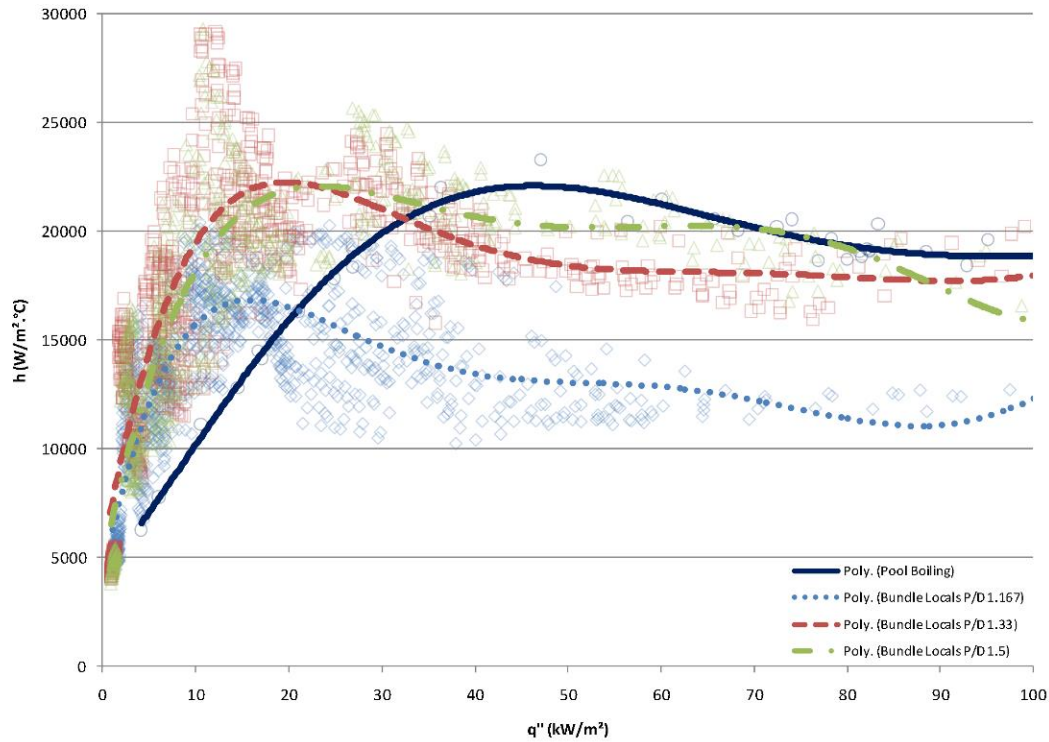


Figure 6 R-134a tube pitch comparison

Effect of mass flux and quality

Figure 7 through Figure 14 present the following comparisons: the heat transfer coefficient vs. heat flux at the same mass flux, heat transfer coefficient vs. heat flux at the same mass flow rate, heat transfer coefficient vs. quality at the same mass flux and heat flux, and heat transfer coefficient vs. quality at the same mass flow rate and heat flux. For the heat transfer coefficient vs. heat flux comparison at 15 and 25 kg/m².s (Figure 7 and Figure 8), P/D 1.33 and P/D 1.5 bundles show similar performance and increasing trend while P/D 1.167 bundle shows a fairly flat trend. For 0.35 and 0.45 kg/s (Figure 9 and Figure 10), P/D 1.33 and P/D 1.5 do not show significant change in performance, but in P/D 1.167, the heat transfer coefficient decreases with the increase in heat flux. For the heat transfer coefficient vs. quality at the same mass flux, mass flow rate, and low heat flux (Figure 11 through Figure 14), P/D 1.33 and P/D 1.5 show an increasing trend, and P/D 1.167 shows a flat trend. For the heat transfer coefficient vs. quality at the same mass flux and medium and high heat fluxes, P/D 1.33 and P/D 1.5 show a near flat trend while P/D 1.167 shows a decreasing trend. The comparison plots clearly show that the bigger tube pitch bundles revealed significantly low heat flux enhancement compared to P/D 1.167. Moreover, both P/D 1.33 and P/D

1.5 demonstrated similar results. Also, this brief parametric study reemphasizes the fact of the prominent heat flux effect on the bundle performance.

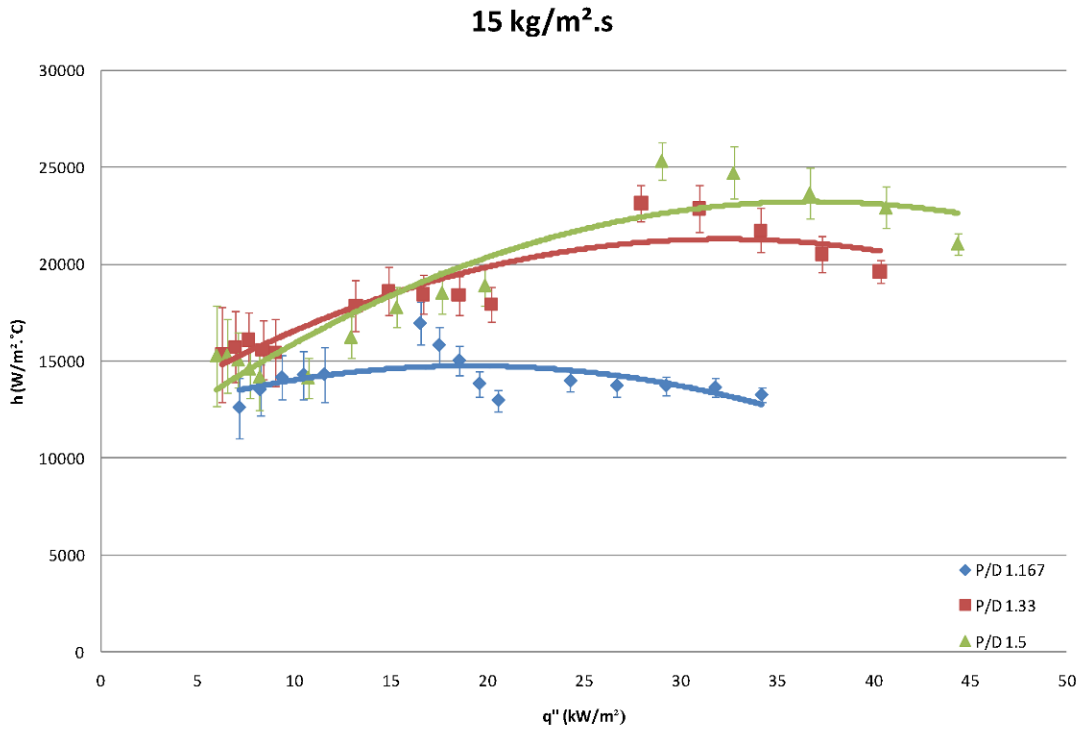
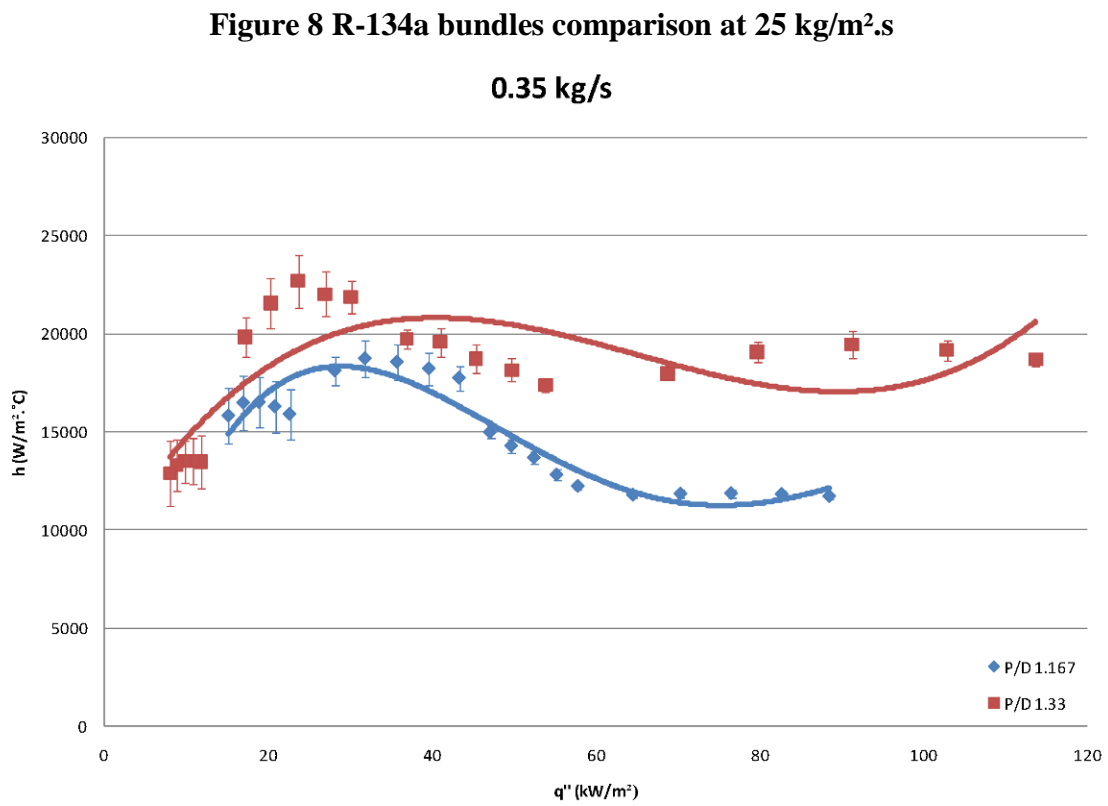
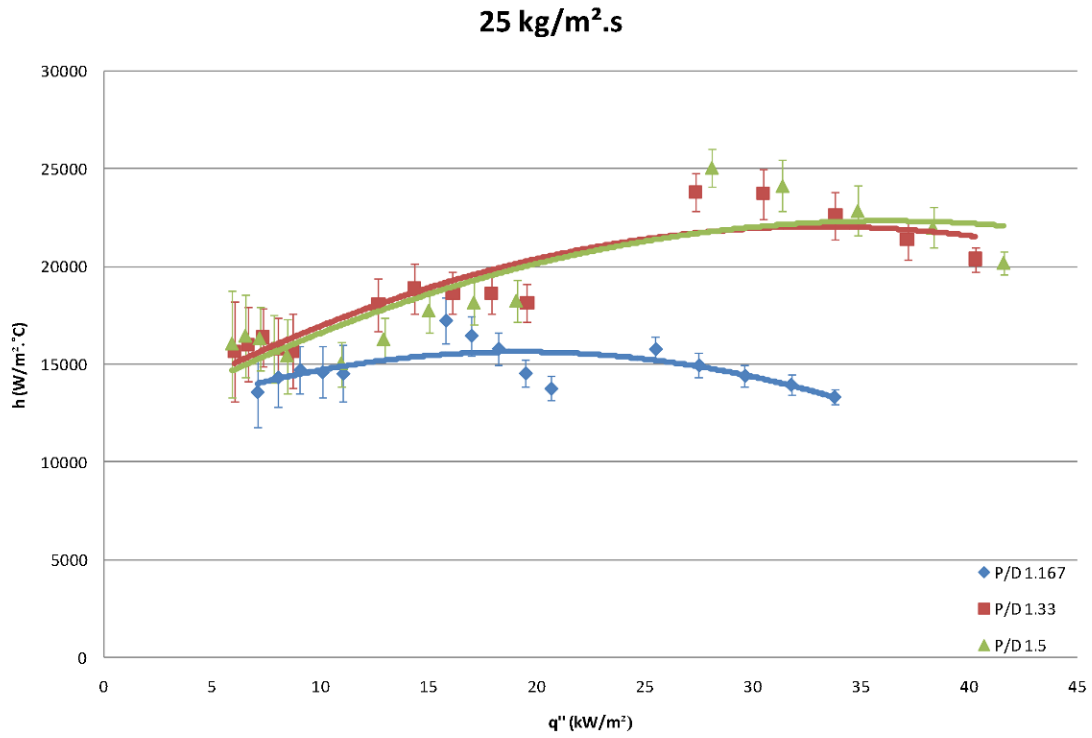


Figure 7 R-134a bundles comparison at 15 kg/m².s



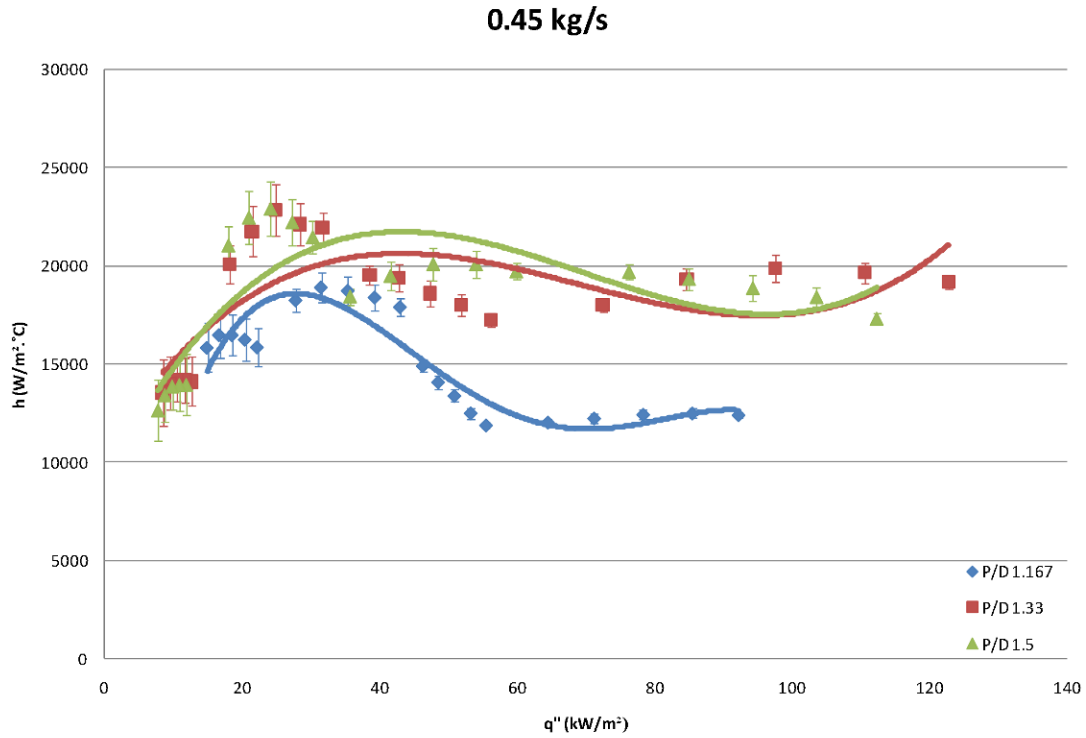


Figure 10 R-134a bundles comparison at 0.45 kg/s

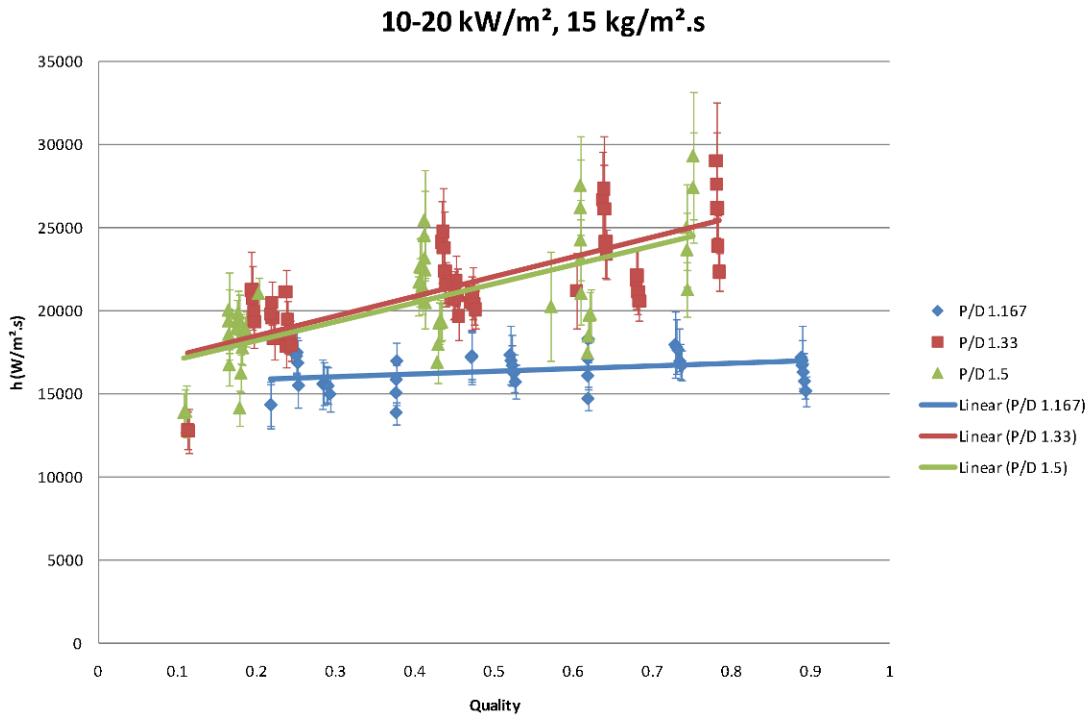


Figure 11 R-134a bundles comparison at 10-20 kW/m² and 15 kg/m².s

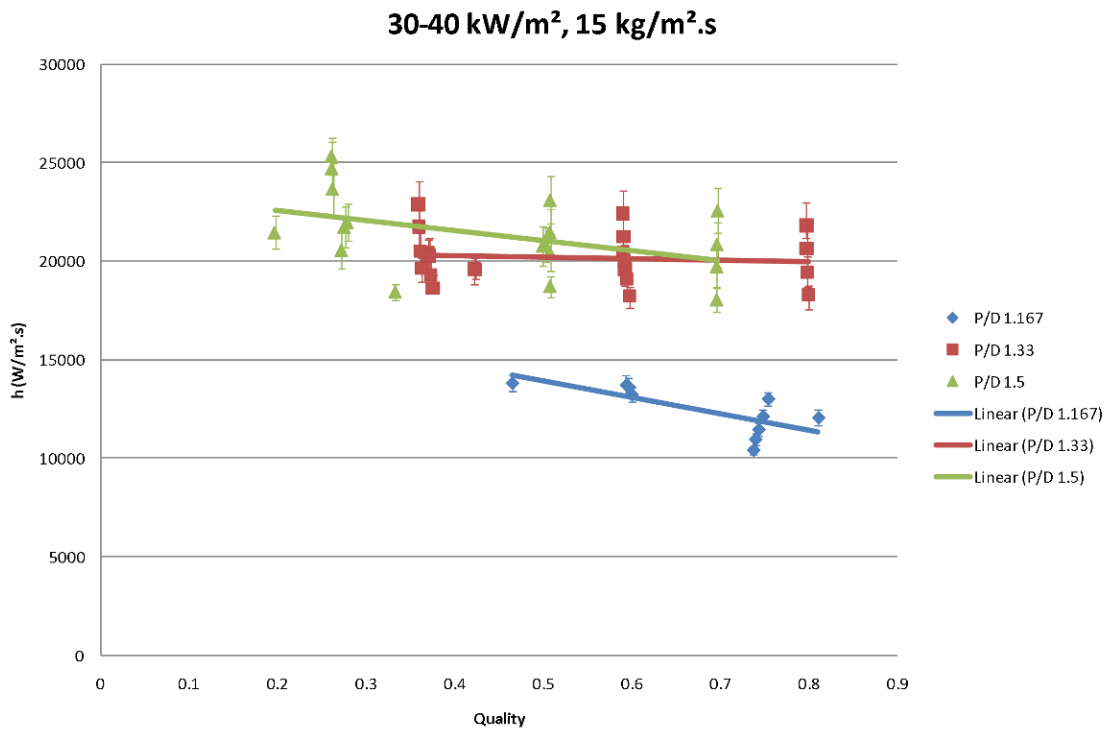


Figure 12 R-134a bundles comparison at 30-40 kW/m² and 15 kg/m².s

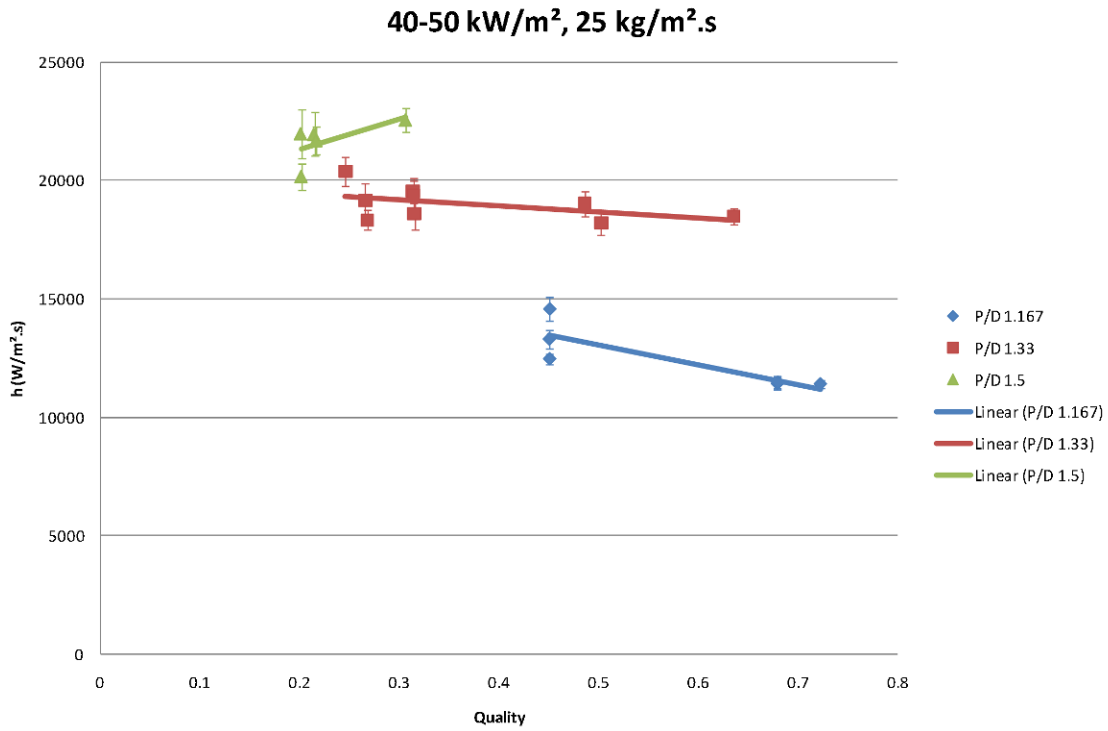


Figure 13 R-134a bundles comparison at 40-50 kW/m² and 25 kg/m².s

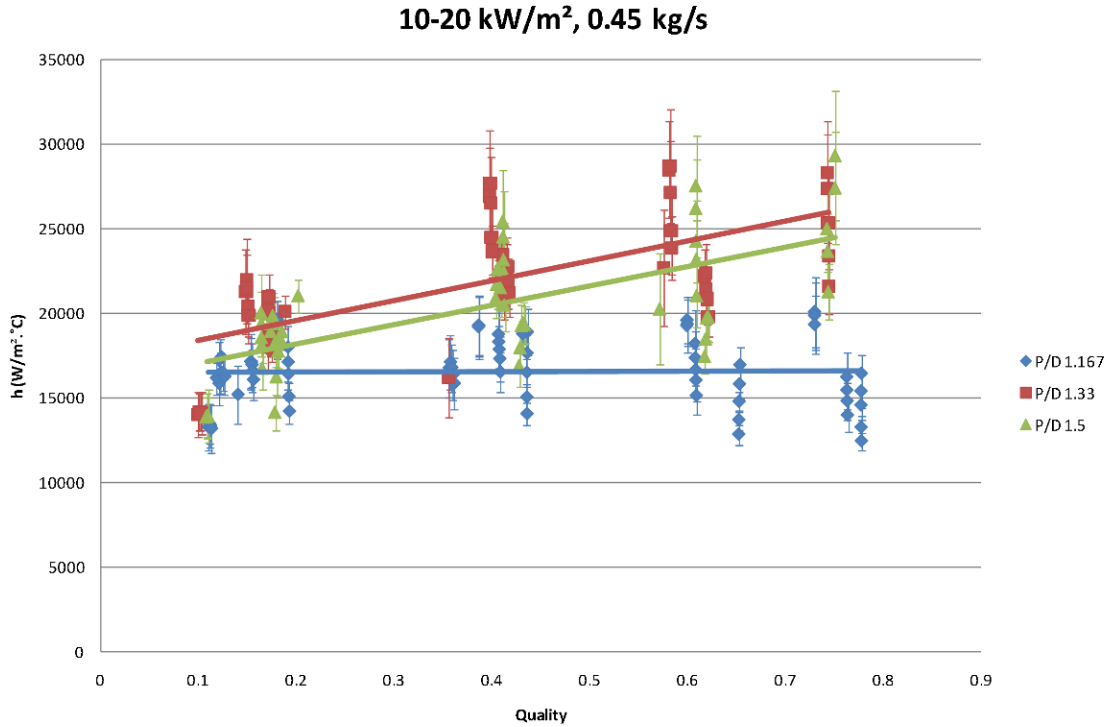


Figure 14 R-134a bundles comparison at 10-20 kW/m² and 0.45 kg/s

Comparison to existing models

Conclusions

This paper presented the experimental local heat transfer coefficient results of convective boiling of R-134a over enhanced tube bundles using TBIHP tubes. Three tube pitches were tested 1.167, 1.33, and 1.5. The analysis used is local to one location in the bundle utilizing the EBHT method in data reduction. Measurements were determined at the minimum flow area between the tubes. Testing was conducted at a saturation temperature of 4.44 °C (40 °F) over a range of heat flux, mass flux, and inlet quality. This investigation reported accurate boiling curves with a clear presentation for the effect of heat flux, mass flux, and local quality on the bundle performance. The results of each tube bundle showed that the dominant parameter in the bundle performance is heat flux. The heat transfer coefficient increases with the increase in quality at low heat flux.

While all bundles showed a rapid increase of performance at low heat flux in comparison to pool boiling, the smallest pitch bundle showed a significantly lower performance than pool boiling. In fact, the heat transfer

coefficient of some points is 1.5 times lower than that of the other two tube pitches. The P/D 1.33 and 1.5 tube bundles showed similar performance with P/D 1.5 slightly higher at medium and high heat flux.

Evidently, the peak performance of the pool boiling curve exists in bundle boiling as well, but is shifted to the left; i.e. at a lower heat flux for convective boiling. All tube bundles experience low heat flux enhancement at the low heat flux range. Since P/D 1.33 and P/D 1.5 have the same low heat flux enhancement, predictably, increasing the tube pitch beyond P/D 1.33 will not increase low heat flux enhancement. Also, as tube pitch increases, the medium and high heat flux region approaches that for the pool boiling performance. This study concludes that the P/D 1.33 is the preferable tube pitch since it provides a considerable performance enhancement over P/D 1.167 and similar enhancement to P/D 1.5. Relatively, the latter is expected to require an increase in refrigerant charge without a notable advantage in performance.

Acknowledgement

This project was sponsored by ASHRAE as RP-1316 “Experimental Evaluation of Heat Transfer Impacts of Tube Pitch in a Highly Enhanced Surface Tube Bundle”. TC 8.5 monitored the program under the chairmanship of Petur Thors. Test tubes were donated by Wolverine Tube, Inc.

Nomenclature

A	Area	P	Pressure
C	Constant	P/D	Pitch to diameter ratio
C_i	Internal correction factor	Pr	Prandtl number
C_p	Specific heat at constant pressure	q''	Heat flux
D	Diameter	Q	Total heat transfer
D_h	Hydraulic diameter	ρ	Density
f	Friction factor	Re	Reynolds number
G	Mass flux	R_{wall}	Wall thermal resistance
h	Heat transfer coefficient	R'_{wall}	$dA_o \cdot R_{wall}$
h_{fg}	Specific heat of vaporization	T	Temperature
i	Enthalpy	T_{sat}	Saturation temperature
k	Thermal conductivity	T_∞	Fluid temperature

k_c	Copper thermal conductivity	U	Overall heat transfer coefficient
L	Length	u	Uncertainty
L_c	Characteristic length	v	Specific volume
\dot{m}	Mass flow rate	x	Quality
Nu	Nusselt number		

References

- Browne, M., and P. Bansal. 1999. Heat transfer characteristics of boiling phenomenon in flooded refrigerant evaporators. *Applied Thermal Engineering* 19(6):595-624.
- Briggs, D.E., and E.H. Young. 1969. Modified Wilson plot techniques for obtaining heat transfer correlations for shell and tube heat exchangers. *Chemical Engineering Progress Symposium Series* 92(65):35-45.
- Casciaro, S., and J.R. Thome. 2001. Thermal performance of flooded evaporators, part 1: Review of boiling heat transfer studies. *ASHRAE Transactions* 107:903-918.
- Collier, J.G., and J.R. Thome. 1996. *Convective boiling and condensation*, 3rd Ed. Oxford University Press, USA.
- Dowlati, R., M. Kawaji, and A. Chan. 1990. Pitch-to-diameter effect on two-phase flow across an in-line tube bundle. *AIChE Journal* 36(5):765-72.
- Fujita, Y., and S. Hidaka. 1998. Effect of tube bundles on nucleate boiling and critical heat flux. *Heat Transfer: Japanese Research* 27(4):312-325.
- Fujita, Y., H. Ohta, S. Hidaka, and K. Nishikawa. 1986. Nucleate boiling heat transfer on horizontal tubes in bundles. *Proceedings of the 8th Int. Heat Transfer Conference* 5:2131-2136.
- Gorgy, E.I., and S. Eckels. 2010. Average heat transfer coefficient for pool boiling of R-134a and R-123 on smooth and enhanced tubes (RP-1316). *HVAC&R* 16(5): 657-676.
- Gorgy, E.I., and S. Eckels. 2012. Local heat transfer coefficient for pool boiling of R-134a and R-123 on smooth and enhanced tubes. *International Journal for Heat and Mass Transfer* 55(11-12): 2751-3326.
- Gnielinski, V. 1976. New equations for heat and mass transfer in turbulent pipe and channel flow. *Int.Chem.Eng* 16(2):359-68.
- Gupta, A. 2005. Enhancement of boiling heat transfer in a 5×3 tube bundle. *International Journal of Heat and Mass Transfer* 48(18):3763-72.
- Hsu, J. -T, and M. K. Jensen. 1988. Effect of pitch-to-diameter ratio on crossflow boiling heat transfer in an inline tube bundle. *Proceedings of ASME, Collected Papers in Heat Transfer* 104:239-245.
- Jensen, M.K., M.J. Reinke, and J.-T. Hsu. 1989. Influence of tube bundle geometry on cross-flow boiling heat transfer and pressure drop. *Experimental Thermal and Fluid Science* 2(4):465-76.
- Jensen, M., and J.T. Hsu. 1988. A parametric study of boiling heat transfer in a horizontal tube bundle. *Journal of Heat Transfer* 110:976.
- Jensen, Michael K., Richard R. Trewin, and Arthur E. Bergles. 1992. Crossflow boiling in enhanced tube bundles. *Proceedings of ASME, Winter Annual Meeting* 220:11-17.
- Kline, S.J., and F. McClintock. 1953. Describing uncertainties in single-sample experiments. *Mechanical Engineering* 75(1):3-8.
- Liao, L., and Z.H. Liu. 2007. Enhanced boiling heat transfer of the compact staggered tube bundles under sub-atmospheric pressures. *Heat Transfer Engineering* 28(5): 444-50.
- Liu, Z.H., and Y.M. Chen. 2001. Enhancement of boiling heat transfer in restricted spaces in compact horizontal tube bundles. *Heat Transfer—Asian Research* 30(5):394-401.
- Liu, Z.H., and Y.H. Qiu. 2002. Enhanced boiling heat transfer in restricted spaces of a compact tube bundle with enhanced tubes. *Applied Thermal Engineering* 22(17):1931-41.
- Liu, Z.H., and Y.H. Qiu. 2004. Boiling heat transfer enhancement of water/salt mixtures on roll-worked enhanced tubes in compact staggered tube bundles. *Chemical Engineering and Technology* 27(11):1187-94.
- Liu, Z.H., and Y.H. Qiu. 2004. Boiling characteristics of R-11 in compact tube bundles with smooth and enhanced tubes. *Experimental heat transfer* 17(2):91-102.
- Liu, Z., and L. Liao. 2006. Enhancement boiling heat transfer study of a newly compact in-line bundle evaporator under reduced pressure conditions. *Chemical Engineering and Technology* 29(3):408-13.

- Liu, Z., and T. Tong. 2002. Boiling heat transfer of water and R-11 on horizontally smooth and enhanced tubes enclosed by a concentric outer tube with two horizontal slots. *Experimental Heat Transfer* 15(3):161-75.
- Memory, S., et al. 1994. Nucleate pool boiling of a TURBO-B bundle in R-113. *Journal of Heat Transfer* 116(3):670-8.
- Memory, S.B., SV Chilman, and PJ Marto. 1992. Nucleate boiling characteristics of a small enhanced tube bundle in a pool of R-113. *28th National Heat Transfer Conference and Exhibition* 129-138.
- Muller, J. 1986. Boiling heat transfer on finned tube bundles—the effect of tube position and intertube spacing. *Proceedings of the 8th International Heat Transfer Conference* 4:2111-2116.
- Petukhov, B. 1970. Heat transfer and friction in turbulent pipe flow with variable physical properties. *Advances in Heat Transfer* 6:503-64.
- Qiu, Y., and Z. Liu. 2004. Boiling heat transfer of water on smooth tubes in a compact staggered tube bundle. *Applied Thermal Engineering* 24(10):1431-41.
- Ribatski, G., and J.R. Thome. 2007. Two-phase flow and heat transfer across horizontal tube bundles—a review. *Heat Transfer Engineering* 28(6):508-24.
- Thome, J.R. 1990. Enhanced boiling heat transfer Hemisphere Pub. Corp.
- Thome, J.R. 1996. Boiling of new refrigerants: A state-of-the-art review. *International Journal of Refrigeration* 19(7): 435-57.
- Thome, J. 1998. Boiling and evaporation of fluorocarbon and other refrigerants: A state-of-the-art review. *Air-Conditioning and Refrigeration Institute (ARI), Arlington, Virginia.*
- Webb, R.L., and N-H Kim. 2005. *Principles of enhanced heat transfer*, 2nd Ed. Taylor & Francis, LLC